intrinsic and extrinsic factors [14]. Glycoprotein (gp)130-stimulating cytokines, such as ciliary neurotrophic factor (CTNF), interleukin (IL)-6 and leukemia inhibitory factor (LIF) are regarded as important factors for neural differentiation in the developing central nervous system [2,29] and in the retina [20,22]. On the other hand, *N*-methyl-D-aspartate (NMDA) induces glutamate receptor-related neurotoxicity in the retina [13], and NMDA-treated eyes have been used as a model for retinal diseases and glaucoma [1,8,10]. In diseased eyes following NMDA-treatment [8], as well as in ischemic retinas [9] or in conditions following mechanical injury [3,32], the up-regulated expression of ciliary neurotrophic factor (CNTF), a gp130-stimulating cytokine, has been demonstrated. Taken together, following transplantation into diseased (NMDA-treated) eyes, the differentiation of transplanted NPCs may be altered by the up-regulated expression of gp130-stimulating cytokines.

Herein, we will report that, in NMDA-treated retinas, transplanted NPCs preferentially differentiate into the glial lineage, and that gp-130 signaling plays an important role in the differentiation after transplantation.

2. Materials and methods

2.1. Culture of neural progenitor cells (NPCs)

NPCs were prepared from the telencephalic neuroepithelium of enhanced green fluorescence protein (EGFP) transgenic mice [19] on embryonic day (E) 14.5. NPCs have the potential to differentiate into neural or glial lineages [2,17]. The isolation and cultivation of NPCs were performed as previously described [17]. In brief, dissociated cells were cultured on poly-L-ornithine (Sigma, St. Louis, MO)/bovine fibronectin (Nitta Gelatin, Osaka, Japan)-coated dishes using a 1:1 mixture of Dulbecco's Modified Eagle's Medium/Ham's F12 (DMEM/F12; Gibco/BRL, Rockville, MD) supplemented with N2 (Sigma) and 10 ng/ml basic fibroblast growth factor (bFGF; R&D System, Minneapolis, MN) for 4 days. Cells were then detached in Hank's balanced salt solution (HBSS), reseeded into culture vessels and grown in the aforementioned medium containing 10 ng/ml bFGF and 10 ng/ml epidermal growth factor (EGF; R&D System) on hydroxyethyl methacrylate (Hema)-coated dishes. Neurospheres formed within 3–5 days.

2.2. Host animals (retinal damage models)

Experiments were performed on adult male Sprague–Drawley rats (6-weeks-old, weight 180–200 g), which were housed at room temperature on a 12-h light/dark cycle while given water and food ad libitum. The retinal damage model was created in a manner similar to that previously described by Morizane et al. [16]. Briefly, rats were anesthetized by intramuscular injection of xylazine (10 mg/kg) and ketamine (20 mg/kg). Pupils were dilated with drops of phenylephrine hydrochloride and tropicamide and a single dose of 5 μl of 4 mM NMDA (total 20 nmol; Sigma) was injected into the vitreous cavity using a microsyringe fitted with a 33-gauge needle. All studies were conducted in accordance with the ARVO Statement for Use of Animals in Ophthalmic and Vision Research.

2.3. Transplantation of NPCs into NMDA-treated eyes

Neurospheres of NPCs were trypsinized, and suspended at 1×10^5 cells/μl in DMEM/F12 supplemented with N2. At 1 day after NMDA injection, 5.0 μl of cell suspension (containing 5×10^5 cells) was slowly injected into the vitreous cavity of the host using a microsyringe fitted with a 33-gauge needle. For immunosuppression, 10 mg/kg of cylosporine A (Wako, Osaka, Japan) was injected subcutaneously every day.

2.4. Tissue sectioning

Animals were sacrificed by an intraperitoneal overdose injection of pentobarbital at 1, 2 and 4 weeks after transplantation. Eyes were enucleated and eyecups were directly immersed in 4% paraformaldehyde for 1 h. The anterior segment and lens were subsequently removed. Posterior eyecups were immersed in the same fixative for 24 h at 4 °C and then in 15%, 20% and 25% sucrose-PBS for cryoprotection. Specimens were embedded in optimal cutting temperature (OCT) compound (Sakura, Tokyo, Japan), and 20-μm frozen sections were made using a cryostat (Leica, Heidelberg, Germany).

2.5. Immunohistochemistry

Specimens were washed with 0.1 M PBS, then incubated in 0.1 M PBS containing 5% skim milk (Nacalai Tesque, Kyoto, Japan) and 2% goat serum (Jackson Immuno Research, West Grove, PA) for 30 min to block nonspecific antibody binding. Samples were then incubated with primary antibodies diluted in 0.1 M PBS containing 5% skim milk for 24 h at 4 °C in a humid chamber. A description of the primary antibodies used follows. Mouse monoclonal anti-nestin (1:200; BD Pharmingen, San Diego, CA) was used as an immature undifferentiated cell marker. Mouse monoclonal anti-GFAP (1:500; Sigma) and rabbit polyclonal anti-GFAP (1:500; Dako, Glostrup, Denmark) were used as markers for astrocytes and reactive Müller glia of the retina. Mouse monoclonal anti-β-tubulin isotype III (1:100; Sigma) was used as a marker for mature neural cells, ganglion cells and amacrine cells of the retina. Mouse monoclonal anti-syntaxin (1:200; Sigma) was used as a marker for amacrine cells of the retina. Mouse monoclonal anti-glutamine synthetase (1:200; Chemicon, Temecula, CA) was used as a marker for Müller glia and

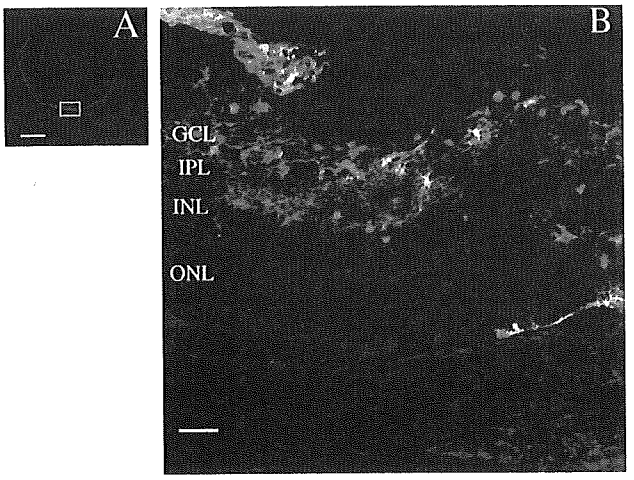

Fig. 1. Confocal image of grafted NPCs in NMDA-damaged retina. Grafted cells were identified through the expression of EGFP (green). Incorporation of cells tended to occur at specific focal points (A: square). All incorporated cells were located in the retinal layer, mostly in GCL and the IPL. Most cells displayed elongated processes. Scale bar, (A) 400 μm; (B) 40 μm. GCL: ganglion cell layer; IPL: inner plexiform layer; INL: inner nuclear layer; ONL: outer nuclear layer.

mouse monoclonal anti-rhodopsin (1:200; LSL, Tokyo, Japan) was used as a marker for rod photoreceptor cells. Rabbit polyclonal antibody to CNTF (Chemicon International, Temecula, CA) was used to determine whether the expression of CNTF was up-regulated in the host retina following NMDA injection or transplantation of NPCs. Following the reaction with primary antibodies, specimens were washed with 0.1 M PBS and incubated with secondary antibody in 0.1 M PBS for 2 h. The secondary antibodies used were Cy3-conjugated goat anti-mouse IgG (1:200, Jackson Immuno Research), rhodamine-conjugated donkey anti-rabbit IgG (1:200, Chemicon) and fluorescein (FITC)-conjugated goat anti-mouse IgG (1:200, Jackson Immuno Research). Sections were then washed with 0.1 M PBS, mounted with Aquatex (Merck, Darmstadt, Germany) and subsequently examined by laser scanning confocal microscopy (FV00, Olympus, Tokyo, Japan).

2.6. Preparation of NPCs from gp130−/− mice

Neuroepithelial cells were cultured from gp130−/− mice in an effort to determine whether glial activation of host retina can affect the differentiation of NPCs. In these cells, gp130-signaling is completely absent. As above, dissociated neuroepithelial cells were derived from telencephalons of gp130−/− and littermate gp130−/− mice at E14.5.

Cells were cultured for 4 days and the GFP marker gene was then transduced using a retroviral vector derived from an MMLV-based viral vector. Cells were detached and replated on a 10-cm dish that had been precoated with poly-L-ornithine/bovine fibronectin at a density of 1×10^6 cells/well. Following the addition of retroviral supernatants, cells were cultured for 2 days, dissociated for transplantation and neurospheres were formed.

2.7. Cell fate analysis and immunofluorescence of NPCs from gp130−/− mice, transplanted into NMDA-treated retinas

One day following NMDA injection, 5.0 μl of cell suspension in DMEM/F12 supplemented with N2 (containing 5×10^5 cells/5.0 μl) was injected according to the methods described. Incorporation and differentiation of the gp130−/− NPC-transduced GFP gene were investigated by immunostaining tissue sections at 2 weeks after transplantation. Eyes were enucleated and tissue sections were stained using rabbit polyclonal anti-GFP and mouse monoclonal anti-GFAP (1:500; Sigma) or mouse monoclonal anti-β-tubulin isotype III (1:100; Sigma) or mouse monoclonal anti-microtubule-associated protein (MAP) (2a + 2b + 2c) (1:500; Sigma) as a marker for neuronal lineage cells.

2.8. Statistical analysis

A Mann–Whitney *U* test was used to compare the mean percentage of GFAP, MAP2 and βIII-tubulin in gp130+/+ mice and gp130−/− mice. A *P* value that was less than 0.05 was considered statistically significant.

3. Results

3.1. Incorporation of NPCs into NMDA-treated retina

In NMDA (20 nmol)-injected eyes, significant cell loss in the ganglion cell layer (GCL) and thinning of the inner plexiform layer (IPL) were observed, as previously observed [8,10]. Transplanted NPCs in host retinas were readily identified by the expression of EGFP [19]. The incorporation of transplanted NPCs in NMDA-treated retinas at 1, 2 and 4 weeks after transplantation was observed in 6/10 eyes (60%), 6/10 eyes (60%) and 7/10

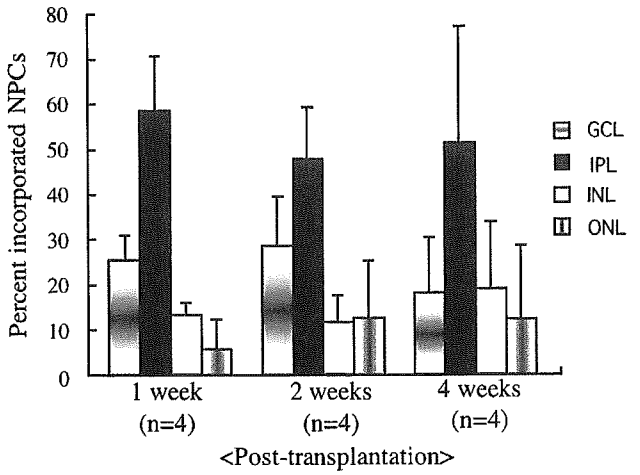

Fig. 2. Proportion of grafted NPCs in host retina. Grafted NPCs were all found in retinal layers, mostly in the GCL and IPL.

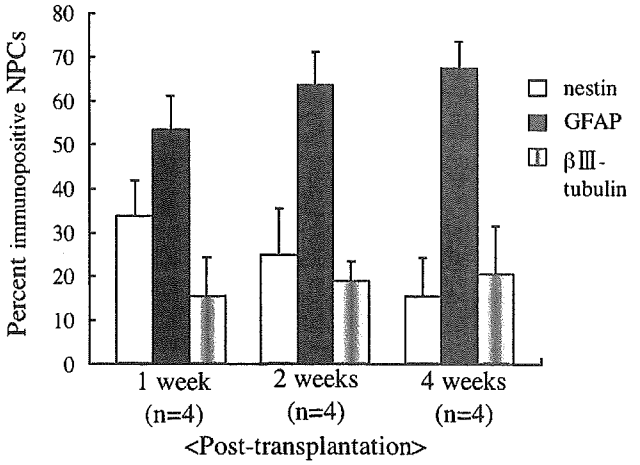

Fig. 3. Proportion of nestin, GFAP and βIII-tubulin immunoreactivity of NPCs. The proportion of nestin-positive NPCs decreased following transplantation. The proportion of GFAP-positive NPCs was almost 3-fold higher than βIII-tubulin-positive NPCs, suggesting preferential differentiation into glial cells.

eyes (70%), respectively. Conversely, no incorporation of transplanted NPCs into adult rat retinas was observed in control experiments without NMDA-treatment, as examined at least 1 and 2 weeks after transplantation (with an intravitreal injection of cell suspension) ($n = 5$).

Following transplantation, the incorporated NPCs migrated to focal areas of the NMDA-treated retina and were found in all retinal layers without detectably affecting the host retinal microstructure (Fig. 1). Morphometric analysis-derived mean percentage of transplanted NPCs in the GCL, IPL, INL and outer nuclear layer (ONL) determined at 1, 2 and 4 weeks after transplantation is summarized in Fig. 2. Four weeks following transplantation, most of the incorporated NPCs were found in the inner retinal layers (GCL and IPL), where NMDA-damage would occur.

3.2. Preferential glial differentiation of transplanted NPCs in NMDA-treated retinas

The mean percentage (±standard deviation) of nestin-positive (immature undifferentiated) cells among transplanted cells at 1, 2 and 4 weeks after transplantation was 33.5 ± 8.1%, 24.7 ± 10.7% and 12.7 ± 3.9%, respectively. The decreased incidence of nestin-positive cells following transplantation suggested that transplanted NPCs differentiated into a mature state over the course of 1 month (Figs. 3, 4A).

In NMDA-treated retinas, the mean percentage of GFAP-positive (glial) cells among transplanted cells at 1, 2 and 4 weeks after transplantation was 53.3 ± 7.6%, 63.5 ± 7.4% and 67.2 ± 6.1%, respectively. Additionally, the mean percentage of βIII-tubulin-positive (mature neuronal) cells among transplanted cells at 1, 2 and 4 weeks after transplantation was 15.3 ± 8.7%, 18.8 ± 4.5% and 20.4 ± 11.0%, respectively (Figs. 3, 4B,C). Furthermore, immunoreactivity towards other retinal cell-type markers such as glutamine synthetase and syntaxin was observed among the transplanted cells (Figs. 4D,E). However, immunoreactivity to rhodopsin was not demonstrated in any of the tissue sections examined, suggesting that transplanted NPCs did not differentiate into rod photoreceptor cells (Fig. 4F).

3.3. Reactive Müller glia in eyes with NMDA-treatments and transplantation of NPCs

At 1 week after NMDA injection, up-regulated immunoreactivity for CNTF was observed in the retina as

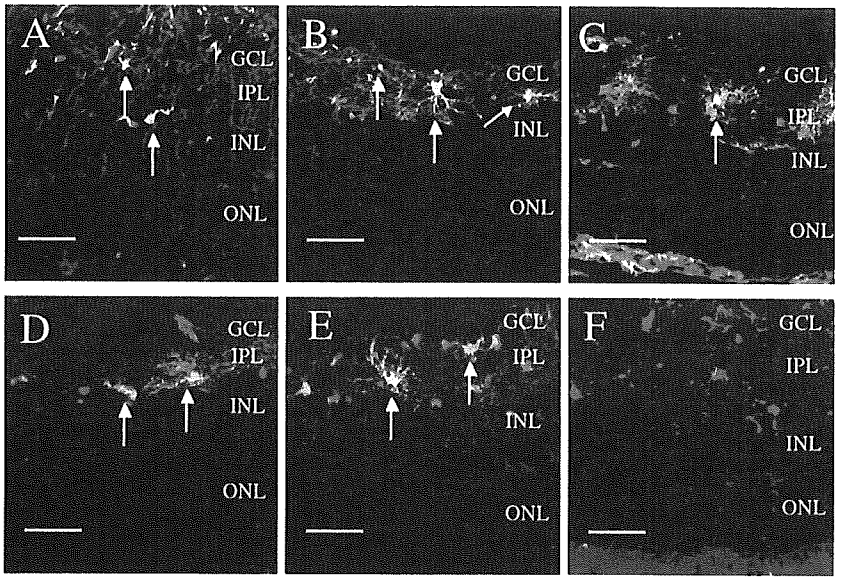

Fig. 4. Confocal images of immunohistochemistry of sections at 2 weeks after NPCs-transplantation. Green: Grafted NPCs (EGFP); Red: nestin- (A), GFAP- (B), βIII-tubulin- (C), syntaxin (D), glutamine synthetase- (E) and rhodopsin-(F) immunoreactivity; Yellow: double-stained NPCs (arrows). Nestin-, GFAP-, βIII-tubulin-, syntaxin- and glutamine synthetase-immunoreactive NPCs were observed; however, rhodopsin-immunoreactive NPCs were negligibly detected throughout the 4-week period. Scale bar, 40 μm.

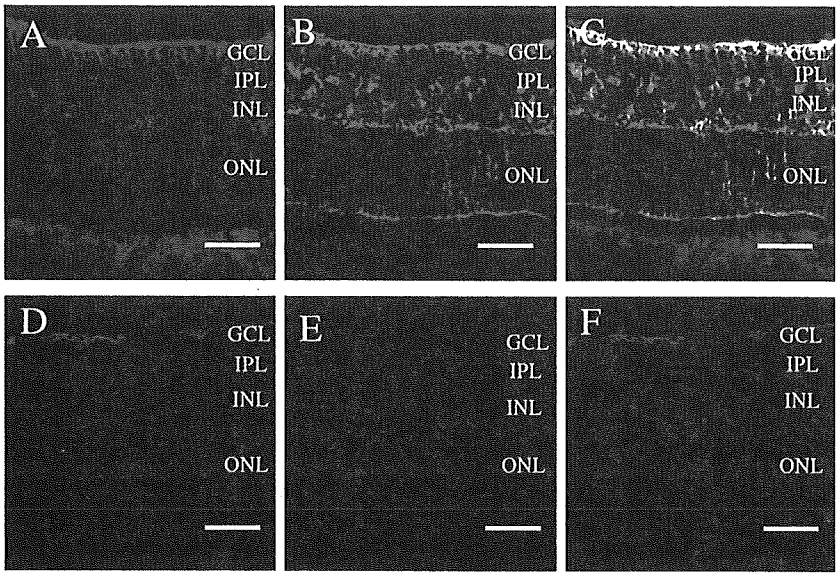

Fig. 5. Double-label immunohistochemistry at 1 week (A–C) and 1 month (D–F) after NMDA injection. Green: immunostained for GFAP (A, C, D and F); Red: immunostained for CNTF (B, C, E and F); Yellow: double-stained (C, F; arrows). Scale bar, 40 μm. Immunoreactivity of GFAP and CNTF in host retina was up-regulated 1 week following NMDA treatment, and then disappeared at 1 month after initial NMDA treatment.

previously described [8]. Up-regulated GFAP immunoreactivity was co-localized with that of CNTF, suggesting that Müller cells were activated (Figs. 5A–C). The expression of GFAP and CNTF decreased concomitantly at 1 month after NMDA injection (Figs. 5D–F). Intense immunoreactivity for GFAP in retinal glial cells in experimental eyes was observed even at 1 month after transplantation of NPCs, suggesting the prolonged presence of activated Müller cells in those eyes (Figs. 6A–C). Additionally, immunohistochemical examination of CNTF revealed that, in NMDA-treated retinas, the immunoreactivity for CNTF was particularly observed in glial cells surrounding the incorporated NPCs (Figs. 6D–F). Noted intensities concerning immunostaining for GFAP and CNTF were observed in retinal glial cells around the transplanted NPCs, unlike the case with NMDA-treated only samples (Figs. 5, 6).

3.4. Inhibited glial differentiation of transplanted NPCs from gp130−/− mice in NMDA-treated retinas

Retinal transplantation experiments using NPCs isolated from gp130−/− mice were conducted. The mean percentage of GFAP-positive cells among the transplanted NPCs was 59.1 ± 6.0% in gp130+/+ mice (n = 3) and 17.6 ± 7.0%

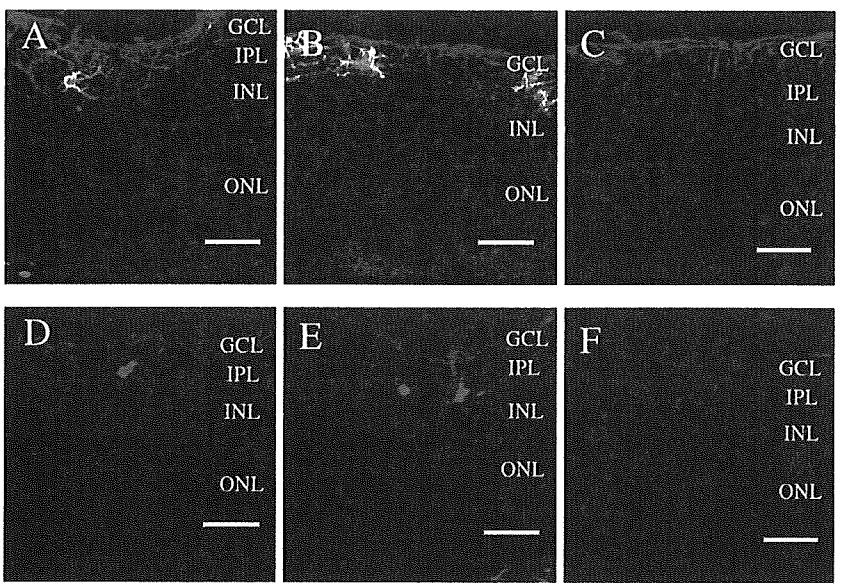

Fig. 6. Confocal microscopy of immunohistochemistry of sections at 1 month after NPC-transplantation. Green: Grafted NPCs (EGFP); Red: GFAP- (A–C), CNTF- (D–F) immunoreactivity. Scale bar, 40 μm. Intense immunoreactivity for GFAP and CNTF in host retinas was observed even 1 month following NPC transplantation.

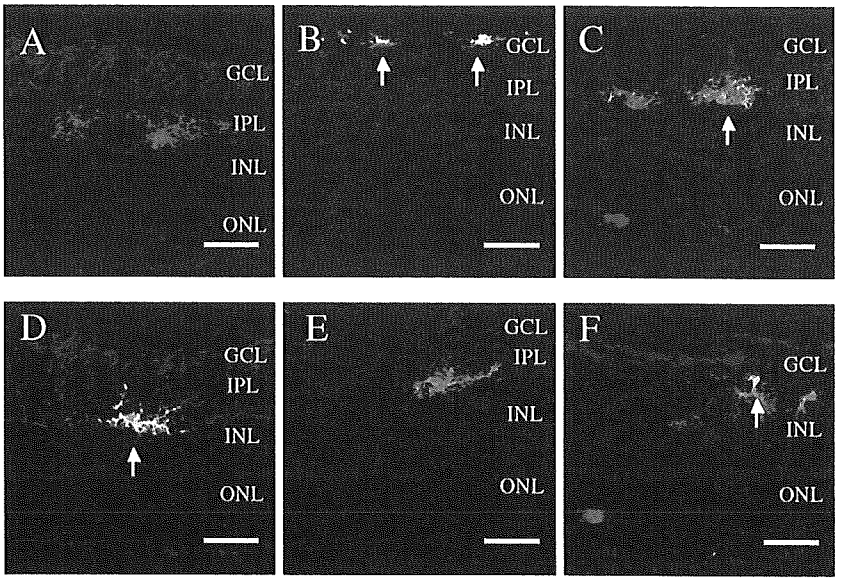

Fig. 7. Double-label immunohistochemistry of NPCs with gp130−/− (A, B and C) or gp130+/+ (D, E and F) following transplantation in NMDA-damaged retinas. Green: Immunostained for GFP (A–G); Red: GFAP- (A and D), MAP2- (B and E), βIII-tubulin- (C and F) immunoreactivity; Yellow: double-stained NPCs (arrows). Immunoreactivity for GFAP was suppressed, while the immunoreactivity for MAP2 was up-regulated in NPCs derived from gp130−/− mice.

(n = 3) in gp130−/− mice, and which showed a statistically significant difference (P = 0.04, Mann–Whitney U test) (Figs. 7, 8). The mean percentage of MAP2-positive NPCs (with neuronal differentiation) was 17.6 ± 5.2% (n = 3) in gp130+/+ and 30.7 ± 6.9% (n = 3) in gp130−/− mice, and showed a statistically significant difference (P = 0.04, Mann–Whitney U test) (Figs. 7, 8). Additionally, the mean percentage of βIII-tubulin-positive NPCs (with mature neuronal differentiation) was 16.3 ± 1.4% (n = 3) in gp130+/+ mice and 17.9 ± 0.6% (n = 3) in gp130−/− mice, and suggested no significant difference between the two strains (P = 0.83, Mann–Whitney U test).

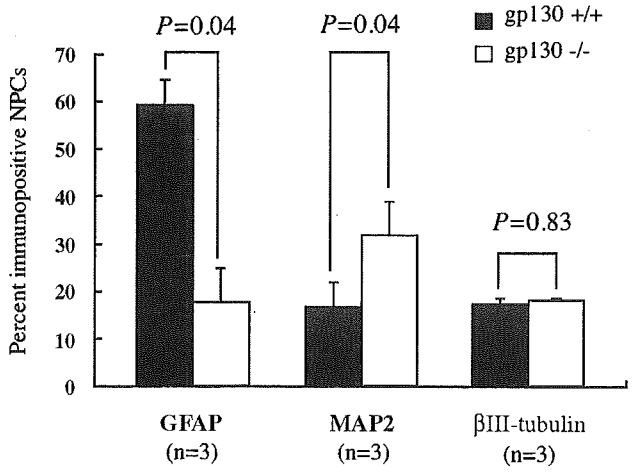

Fig. 8. Mean percentage of GFAP, MAP2 and βIII-tubulin immunoreactivity for NPCs with or without gp130 signaling. The percentage of immunoreactivity for GFAP decreased significantly in NPCs deficient for gp130. In contrast, the percentage of immunoreactivity for MAP2 increased significantly.

4. Discussion

Investigations concerning retinal regenerative therapy have received a great deal of attention since this novel therapeutic concept may present a breakthrough to assist the social activities of blind patients. To achieve the restoration of visual functions, basic knowledge concerning the differentiation of transplanted progenitor cells in the retina is necessary. The development of a transplantation methodology utilizing neuronal progenitor cells could provide us with a basic understanding of key factors related to the determination of cell fate.

Previous studies reported that following injection of a cell suspension into the vitreous cavity, NPCs could incorporate and differentiate into mature retinas with mechanically-induced damage [18] or with transient ischemia [12], and into developing [28] and dystrophic retinas [35]. This could not be achieved in normal mature retina. In our present study, no incorporation of transplanted NPCs into adult rat retinas without NMDA-treatment was observed, which agrees with previous findings [12,18, 28,35]. However, other reports have showed that the embryonic precursor cells are incorporated in the normal adult mouse retina [7,21]. The difference of host retinal microenvironment (mouse or rat) may influence the incorporation of neural progenitor cell. Our results demonstrated a preferential differentiation of incorporated NPCs into the glial lineage. Previous reports have demonstrated the preferential glial differentiation of embryonic brain-derived NPCs transplanted into brain [33], spinal cord [4] and retinas [21,34].

It is well known that common progenitor cells can differentiate into neuronal or glial lineages [30]. The

molecular mechanisms associated with the determination of progenitor cell lineage in retinas are thought to be stimulated by a series of intrinsic and extrinsic factors [14]. Among the known key factors that determine cell lineage, gp130-stimulating cytokines are regarded as important factors. These preferentially determine the cell fate of progenitors into the glial lineage. To date, gp130-stimulating cytokines comprise a group of factors including LIF, interleukin (IL)-6, IL-11, oncostain-M, cardiotrophin-1 and ciliary neurotrophic factor (CNTF) [26,27]. All these cytokines use gp130 in their respective receptor complexes as a signal transduction component [11,23–25,27]. In diseased eyes, some members of the gp130-stimulating cytokines have been found in the retina and vitreous [3,8,9,32]. In our previous study, the up-regulated expression of CNTF produced from activated Müller cells was demonstrated in NMDA-treated retinas [8]. In this study, immunohistochemical analysis revealed a prolonged and intense expression of CNTF in host retinal glial cells when NPCs were incorporated into the host retina. Taken together, we hypothesized that the up-regulated expression of gp130-stimulating cytokines (including CNTF) in activated host glial cells may therefore induce glial differentiation of transplanted NPCs.

In an effort to examine our hypothesis regarding a relationship between gp130 signaling and glial differentiation in transplanted NPCs, gp130−/− mice were used. Our results revealed a significant decrease in GFAP-positive (glial) cells among the transplanted gp130−/− mice-derived NPCs in NMDA-treated retinas. In contrast, in experiments using gp130−/− mice-derived NPCs, the percentage of MAP2-positive cells increased significantly compared to wild-type littermates. MAP2-positive cells are thought to represent immature neuronal cells [5]. These findings showed that gp130-signaling plays an important role in the differentiation of transplanted NPCs.

In conclusion, our results revealed that, in NMDA-treated retinas, transplanted NPCs preferentially differentiate into the glial lineage through a gp130-signaling pathway.

Acknowledgments

The authors thank Dr. K. Yoshida and Dr. T. Kishimoto for providing the gp130 mutant mice.

References

[1] K. Adachi, Y. Fujita, C. Morizane, A. Akaike, M. Ueda, M. Satoh, H. Masai, S. Kashii, Y. Honda, Inhibition of NMDA receptors and nitric oxide synthase reduces ischemic injury of the retina, Eur. J. Pharmacol. 350 (1998) 53–57.

[2] A. Bonni, Y. Sun, M. Nadal-Vicens, A. Bhatt, D.A. Frank, I. Rozovsky, N. Stahl, G.D. Yancopoulos, M.E. Greenberg, Regulation of gliogenesis in the central nervous system by the JAK-STAT signaling pathway, Science 278 (1997) 477–483.

[3] W. Cao, R. Wen, F. Li, M.M. Lavail, R.H. Steinberg, Mechanical injury increases bFGF and CNTF mRNA expression in the mouse retina, Exp. Eye Res. 65 (1997) 241–248.

[4] Q.L. Cao, Y.P. Zhang, R.M. Howard, W.M. Walters, P. Tsoulfas, S.R. Whittemore, Pluripotent stem cells engrafted into the normal or lesioned adult rat spinal cord are restricted to a glial lineage, Exp. Neurol. 167 (2001) 48–58.

[5] M. Goedert, R.A. Crowther, C.C. Garner, Molecular characterization of microtubule-associated proteins tau and MAP2, Trends Neurosci. 14 (1991) 193–199.

[6] Y. Guo, P. Saloupis, S.J. Shaw, D.W. Rickman, Engraftment of adult neural progenitor cells transplanted to rat retina injured by transient ischemia, Invest. Ophthalmol. Visual Sci. 44 (2003) 3194–3201.

[7] A. Hara, M. Niwa, T. Kunisada, N. Yoshimura, M. Katayama, O. Kozawa, H. Mori, Embryonic stem cells are capable of generating a neuronal network in the adult mouse retina, Brain Res. 999 (2004) 216–221.

[8] M. Honjo, H. Tanihara, N. Kido, M. Inatani, K. Okazaki, Y. Honda, Expression of ciliary neurotrophic factor activated by retinal Muller cells in eyes with NMDA- and kainic acid-induced neuronal death, Invest. Ophthalmol. Visual Sci. 41 (2000) 552–560.

[9] W.K. Ju, M.Y. Lee, H.D. Hofmann, M. Kirsch, M.H. Chun, Expression of CNTF in Muller cells of the rat retina after pressure-induced ischemia, NeuroReport 10 (1999) 419–422.

[10] N. Kido, H. Tanihara, M. Honjo, M. Inatani, T. Tatsuno, C. Nakayama, Y. Honda, Neuroprotective effects of brain-derived neurotrophic factor in eyes with NMDA-induced neuronal death, Brain Res. 884 (2000) 59–67.

[11] T. Kishimoto, T. Taga, S. Akira, Cytokine signal transduction, Cell 76 (1994) 253–262.

[12] Y. Kurimoto, H. Shibuki, Y. Kaneko, M. Ichikawa, T. Kurokawa, M. Takahashi, N. Yoshimura, Transplantation of adult rat hippocampus-derived neural stem cells into retina injured by transient ischemia, Neurosci. Lett. 306 (2001) 57–60.

[13] D.R. Lucas, J.P. Newhouse, The toxic effect of sodium L-glutamate on the inner layers of the retina, AMA Arch. Ophthalmol. 58 (1957) 193–201.

[14] T. Marquardt, P. Gruss, Generating neuronal diversity in the retina: one for nearly all, Trends Neurosci. 25 (2002) 32–38.

[15] H. Mizumoto, K. Mizumoto, M.A. Shatos, H. Klassen, M.J. Young, Retinal transplantation of neural progenitor cells derived from the brain of GFP transgenic mice, Vision Res. 43 (2003) 1699–1708.

[16] C. Morizane, K. Adachi, I. Furutani, Y. Fujita, A. Akaike, S. Kashii, Y. Honda, *N*(omega)-nitro-L-arginine methyl ester protects retinal neurons against *N*-methyl-D-aspartate -induced neurotoxicity in vivo, Eur. J. Pharmacol. 328 (1997) 45–49.

[17] K. Nakashima, M. Yanagisawa, H. Arakawa, T. Taga, Astrocyte differentiation mediated by LIF in cooperation with BMP2, FEBS Lett. 457 (1999) 43–46.

[18] A. Nishida, M. Takahashi, H. Tanihara, I. Nakano, J.B. Takahashi, A. Mizoguchi, C. Ide, Y. Honda, Incorporation and differentiation of hippocampus-derived neural stem cells transplanted in injured adult rat retina, Invest. Ophthalmol. Visual Sci. 41 (2000) 4268–4274.

[19] M. Okabe, M. Ikawa, K. Kominami, T. Nakanishi, Y. Nishimune, 'Green mice' as a source of ubiquitous green cells, FEBS Lett. 407 (1997) 313–319.

[20] W.M. Peterson, Q. Wang, R. Tzekova, S.J. Wiegand, Ciliary neurotrophic factor and stress stimuli activate the Jak-STAT pathway in retinal neurons and glia, J. Neurosci. 20 (2000) 4081–4090.

[21] S. Pressmar, M. Ader, G. Richard, M. Schachner, U. Bartsch, The fate of heterotopically grafted neural precursor cells in the normal and dystrophic adult mouse retina, Invest. Ophthalmol. Visual Sci. 42 (2001) 3311–3319.

[22] K.D. Rhee, X.J. Yang, Expression of cytokine signal transduction components in the postnatal mouse retina, Mol. Vision 9 (2003) 715–722.

[23] N. Stahl, G.D. Yancopoulos, The tripartite CNTF receptor complex: activation and signaling involves components shared with other cytokines, J. Neurobiol. 25 (1994) 1454–1466.
[24] T. Taga, IL6 signalling through IL6 receptor and receptor-associated signal transducer, gp130, Res. Immunol. 143 (1992) 737–739.
[25] T. Taga, The signal transducer gp130 is shared by interleukin-6 family of haematopoietic and neurotrophic cytokines, Ann. Med. 29 (1997) 63–72.
[26] T. Taga, T. Kishimoto, Gp130 and the interleukin-6 family of cytokines, Annu. Rev. Immunol. 15 (1997) 797–819.
[27] T. Taga, M. Hibi, Y. Hirata, K. Yamasaki, K. Yasukawa, T. Matsuda, T. Hirano, T. Kishimoto, Interleukin-6 triggers the association of its receptor with a possible signal transducer, gp130, Cell 58 (1989) 573–581.
[28] M. Takahashi, T.D. Palmer, J. Takahashi, F.H. Gage, Widespread integration and survival of adult-derived neural progenitor cells in the developing optic retina, Mol. Cell. Neurosci. 12 (1998) 340–348.
[29] T. Takizawa, M. Yanagisawa, W. Ochiai, K. Yasukawa, T. Ishiguro, K. Nakashima, T. Taga, Directly linked soluble IL-6 receptor-IL-6 fusion protein induces astrocyte differentiation from neuroepithelial cells via activation of STAT3, Cytokine 13 (2001) 272–279.
[30] D.L. Turner, C.L. Cepko, A common progenitor for neurons and glia persists in rat retina late in development, Nature 328 (1987) 131–136.
[31] S.J. Van Hoffelen, M.J. Young, M.A. Shatos, D.S. Sakaguchi, Incorporation of murine brain progenitor cells into the developing mammalian retina, Invest. Ophthalmol. Visual Sci. 44 (2003) 426–434.
[32] R. Wen, Y. Song, T. Cheng, M.T. Matthes, D. Yasumura, M.M. LaVail, R.H. Steinberg, Injury-induced upregulation of bFGF and CNTF mRNAS in the rat retina, J. Neurosci. 15 (1995) 7377–7385.
[33] C. Winkler, R.A. Fricker, M.A. Gates, M. Olsson, J.P. Hammang, M.K. Carpenter, A. Bjorklund, Incorporation and glial differentiation of mouse EGF-responsive neural progenitor cells after transplantation into the embryonic rat brain, Mol. Cell. Neurosci. 11 (1998) 99–116.
[34] A.B. Wojciechowski, U. Englund, C. Lundberg, K. Warfvinge, Long-term survival and glial differentiation of the brain-derived precursor cell line RN33B after subretinal transplantation to adult normal rats, Stem Cells 20 (2002) 163–173.
[35] M.J. Young, J. Ray, S.J. Whiteley, H. Klassen, F.H. Gage, Neuronal differentiation and morphological integration of hippocampal progenitor cells transplanted to the retina of immature and mature dystrophic rats, Mol. Cell. Neurosci. 16 (2000) 197–205.

Molecular Vision 2005; 11:431-7 <http://www.molvis.org/molvis/v11/a50/>
Received 20 October 2004 | Accepted 16 June 2005 | Published 23 June 2005

Association between glaucoma and gene polymorphism of endothelin type A receptor

Karin Ishikawa,[1] Tomoyo Funayama,[1] Yuichiro Ohtake,[1] Itaru Kimura,[1] Hidenao Ideta,[2] Kenji Nakamoto,[3] Noriko Yasuda,[3] Takeo Fukuchi,[4] Takuro Fujimaki,[5] Akira Murakami,[5] Ryo Asaoka,[6] Yoshihiro Hotta,[6] Takashi Kanamoto,[7] Hidenobu Tanihara,[8] Koichi Miyaki,[9] Yukihiko Mashima[1]

Departments of [1]Ophthalmology and [9]Preventive Medicine and Public Health, Keio University School of Medicine, Tokyo, Japan; [2]Ideta Eye Hospital, Kumamoto, Japan; [3]Department of Ophthalmology, Tokyo Metropolitan Police Hospital, Tokyo, Japan; [4]Department of Ophthalmology, Niigata University School of Medicine, Niigata, Japan; [5]Department of Ophthalmology, Juntendo University School of Medicine, Tokyo, Japan; [6]Department of Ophthalmology, Hamamatsu University School of Medicine, Hamamatsu, Japan; [7]Department of Ophthalmology, Hiroshima University School of Medicine, Hiroshima, Japan; [8]Department of Ophthalmology, Kumamoto University School of Medicine, Kumamoto, Japan

Purpose: Endothelin 1 (ET-1), a potent vasoconstrictor, may affect regulation of intraocular pressure and ocular vessel tone. Thus, ET-1 and its receptors may contribute to development of glaucoma. We investigated whether gene polymorphisms of ET-1 (*EDN1*) and its receptors ET_A (*EDNRA*) and ET_B (*EDNRB*) were associated with glaucoma phenotypes and clinical features.

Methods: We studied 224 normal Japanese controls and 426 open angle glaucoma (OAG) patients including 176 with primary open angle glaucoma (POAG) and 250 with normal tension glaucoma (NTG). Nine single nucleotide polymorphisms were detected among the participants using the Invader® assay; four for *EDN1* (T-1370G, +138/ex1 del/ins, G8002A, K198N), four for *EDNRA* (G-231A, H323H, C+70G, C+1222T), and one for *EDNRB* (L277L). Genotype distributions were compared between normal controls and OAG. Age at diagnosis, untreated maximum intraocular pressure (IOP), and visual field defects at diagnosis were examined for association with polymorphisms.

Results: Of the 9 polymorphisms, genotype distributions showed no significant differences between OAG patients and controls adjusted by age. The GG genotype of *EDNRA*/C+70G was associated with worse visual field defects in NTG patients (p=0.014; Mann-Whitney U test, and p=0.027; logistic regression analysis).

Conclusions: The polymorphism of *EDNRA*/C+70G may be related to NTG risk factors.

Glaucoma is the second leading cause of vision loss worldwide. The number of persons with primary glaucoma was estimated at nearly 66.8 million, including 6.7 million with bilateral blindness [1]. Open angle glaucoma (OAG) is a slowly progressive atrophy of the optic nerve characterized by visual field changes corresponding to excavation of the optic disc [2]. OAG, the most common type of glaucoma, is divided into primary open angle glaucoma (POAG), where elevated intraocular pressure (IOP) is above 21 mm Hg, and normal tension glaucoma (NTG), where IOP does not exceed 21 mm Hg. Among Japanese, NTG accounts for 92% of OAG, a higher proportion than in Caucasians [3]. Although an elevated IOP is a major risk factor, the pathophysiology of OAG is not precisely known. OAG is a multifactorial disease that results from interactions between multiple genetic and environmental factors [4]. Both mechanical and vascular mechanisms have been proposed [2,5].

Recent studies have demonstrated that endothelin and its receptors may contribute significantly to development of the optic neuropathy characteristic of glaucoma [6,7]. Endothelin 1 (ET-1), a potent 21-amino acid vasoconstrictive peptide produced by vascular endothelial cells [8,9], is considered the most important vasoconstrictor among three isopeptides identified (the others being endothelin-2 and endothelin-3). Endothelin receptors, type A (ET_A) and type B (ET_B), mediate the biological effects of ET-1. The potent vasoconstrictor effect of ET-1 is mediated predominantly by ET-1 specific ET_A receptors located on vascular smooth muscle cells and, to a lesser extent, by activation of ET_B receptors, which are nonselective among endothelins [10-12].

The presence of the ET system is well established in the eye, where ET and its receptors have been found in most tissues [13-17]. Aqueous humor ET levels were reported to be higher in patients with POAG than in normal subjects [18,19], while Källberg et al. [20] made the same observations in dogs with hypertensive glaucoma compared with healthy dogs.

Although two studies reported significantly higher plasma ET-1 levels in patients with NTG than in normal control subjects [21,22], Tezel et al. [19] found no significant difference in plasma ET levels between POAG patients and controls. Kaiser et al. [23] reported a tendency toward higher plasma ET-1 levels in NTG patients than in POAG patients, although the differences were not statistically significant. They also noted an abnormality in ET-1 production in response to postural

Correspondence to: Karin Ishikawa, MD, Department of Ophthalmology, Keio University School of Medicine, 35 Shinanomachi, Shinjuku-ku, Tokyo 160-8582, Japan; Phone: (+81) 3-3353-1211, ext. 62402; FAX: (+81) 3-3359-8302; email: karin-i@sc.itc.keio.ac.jp

changes in NTG patients. In addition, several reports have suggested that glaucomatous nerve fiber damage was affected by vasospasm [24], systemic vascular endothelial cell dysfunction [25], and microvascular dysfunction [26] mediated by ET-1. Thus, ET-1 has been suggested to participate in regulation of IOP and ocular vessel tone, but is also suspected to take part in the pathogenesis of glaucoma.

Population based association studies using polymorphic candidate genes are one approach to identifying genes conferring increased susceptibility to glaucoma. However, the impact of endothelin related genetic polymorphisms on glaucoma is incompletely determined. One previous association study in Australian Caucasians has reported a possible involvement of the ET-1 gene in glaucoma, finding no alterations in the promoter region of the ET-1 gene [27]. In the present study, we investigated whether gene polymorphisms of ET-1 (*EDN1*), and the receptors ET_A (*EDNRA*) and ET_B (*EDNRB*) were associated with OAG phenotypes and clinical features in a Japanese population.

METHODS

Study population: A total of 650 Japanese subjects (224 normal controls, 176 POAG patients, and 250 NTG patients), recruited from seven Japanese medical institutions, were examined. Blood samples were analyzed at Keio University. All subjects were unrelated. The mean age (±standard deviation) at diagnosis of OAG was 57.2±12.8 years. OAG subjects were divided into POAG patients and NTG patients, aged 58.8±12.2 and 56.1±13.2 years at diagnosis, respectively (Table 1). The mean age at the time of examination was 70.0±11.2 years in controls. We purposely selected older control subjects to reduce the likelihood that a subset of controls would later develop glaucoma.

The procedures used in this human research conformed to the tenets of the Declaration of Helsinki. Written informed consent was obtained after the nature and possible consequences of the study were explained. Where applicable, the research was approved by the Keio Institutional Human Experimentation Committee.

Ophthalmic examinations included slit-lamp biomicroscopy, optic disc examination, IOP measurement by Goldmann applanation tonometry, and gonioscopy. Visual fields were assessed with the Humphrey automated perimetry (program 30-2) or Goldmann perimetry. The severity of the visual field defects was scored from 1 to 5 [28,29]. The data obtained by the two types of perimetry were combined using a five point scale: (1) no alterations, (2) early defects, (3) moderate defects, (4) severe defects, and (5) light perception only or no light perception. This severity scale followed Kozaki's classification [30,31], which has been used most widely in Japan so far, based on Goldmann perimetry or by the classification established for the Humphrey Field Analyzer [32].

Among the patients with OAG, POAG was diagnosed upon fulfillment of all of the following criteria; maximum IOP was above 21 mm Hg, open angles on gonioscopy, typical glaucomatous disc cupping associated with visual field changes, and absence of other ocular, rhinologic, neurological, or systemic disorders potentially causing optic nerve damage. We excluded patients with elevated IOP secondary to defined causes (e.g., trauma, uveitis, steroid administrtion, or exfoliative, pigmentary, or neovascular glaucoma). POAG patients with *MYOC* or *OPTN* mutations and juvenile OAG patients were also excluded. Among the patients with OAG, NTG was diagnosed by the same criteria as POAG except that IOP did not exceed 21 mm Hg at all times, including the three baseline measurements and during the diurnal test (IOP every 3 h from 6 AM to 24 PM), when the peak IOP with or without medication after diagnosis was consistently below 22 mm Hg throughout the follow-up period. Normal control subjects had IOP less than 20 mm Hg, no glaucomatous disc changes, and no family history of glaucoma.

DNA extraction and genotyping of the polymorphisms: Genomic DNA was isolated from peripheral blood lymphocytes by standard methods. Nine single nucleotide polymorphisms (SNPs) were detected among all participants; four for *EDN1* (T-1370G, +138/ex1 del/ins, G8002A, K198N), four for *EDNRA* (G-231A, H323H, C+70G, C+1222T), and one for *EDNRB* (L277L). These polymorphisms are listed at GeneCanvas. We genotyped these SNPs using the Invader® assay (Third Wave Technologies, Inc., Madison, WI), which was recently developed for high throughput genotyping of SNPs [33]. The oligonucleotide sequences of primary probes and Invader® probes used in this study are listed in Table 2.

Statistical analysis: Comparisons of genotype distributions in normal controls with those in OAG patients were performed by χ^2 analysis. Age adjustments were also performed using logistic regression analysis. Associations of clinical characteristics (age at diagnosis, untreated maximum of IOP, and visual field score at diagnosis) with genotypes were assessed by the Mann-Whitney U test. Multivariate analyses were also performed with a logistic regression model to confirm the association between these clinical characters and the genotypes. Statistical analyses were carried out with SPSS for Windows (version 12.0; SPSS Inc., Chicago, IL). A value of $p<0.05$ was considered to be significant.

TABLE 1. CHARACTERISTICS OF SUBJECTS

Sample	Age at diagnosis (years)	Gender (male/female)	Systemic hypertension	Family history of glaucoma	Untreated maximum IOP (mm Hg)	Visual field score at diagnosis
Control (n=224)	70.0±11.2	100/124	53 (23.7)	(0.0)		1.0±0.0
POAG (n=176)	58.8±12.2	100/ 76	43 (24.4)	56 (33.0)	26.8±6.1	3.1±0.9
NTG (n=250)	56.1±13.2	119/131	51 (20.4)	91 (32.4)	16.9±2.2	2.8±0.

A total of 650 Japanese subjects were examined. We purposely selected older control subjects to reduce the likelihood that a subset of this group would later develop glaucoma. No significant difference was observed in prevalence of systemic hypertension between POAG, NTG, and control groups. Data for age at diagnosis, maximum IOP, and visual field score are expressed as means±standard deviation. Data for systemic hypertension and history of glaucoma are counts with percentages in parentheses.

RESULTS

Table 3 shows genotype and allele frequencies obtained in this study. The distributions in control and OAG were consistent with the Hardy-Weinberg equilibrium. For the *EDN1*/+138/ex1 del/ins polymorphism, the frequencies of the del/del and del/ins+ins/ins genotypes, respectively, were 74.2% and 25.8% in OAG patients (p=0.016), compared with 65.2% and 34.8% in control subjects. For the *EDN1*/K198N polymorphism, 53.2% of OAG patients were found to have the KK genotype, which tended to be higher than the 43.8% in control subjects (p=0.022). For the *EDNRA*/C+1222T polymorphism, the frequency of the CT+TT genotype in OAG patients tended to be higher than in control subjects (p=0.036). However, when adjusted by age, these case-control studies did not reveal significant differences between OAG patients and controls. Adjusted p values are shown in Table 3. Polymorphism of *EDN1*/G8002A in the intron 4 region was highly coincident with *EDN1*/K198N (data not shown).

Characteristics of patients were examined for a dominant model and a recessive model for each polymorphism, and data with significant differences are shown in Table 4. In all OAG patients and in POAG patients, no characteristic showed a significant difference between genotype groups. In NTG patients, however, we found significantly poorer visual field scores at diagnosis in the GG group for *EDNRA*/C+70G than the CC+CG group (3.0±0.7 compared to 2.7±0.7, p=0.014; Mann-Whitney U test). Because these three characteristics (age at diagnosis, untreated maximum IOP, and visual field defects at diagnosis) may be linked, the relationships between genotypes were investigated by logistic regression analysis. It still revealed significantly poorer visual field scores in the GG group than the CC+CG group (p=0.027). Other polymorphisms in NTG patients showed no significant differences in characteristics between genotype groups.

DISCUSSION

Considerable evidence has been collected implicating vascular insufficiency as the cause of glaucomatous nerve fiber damage [24-26,34]. IOP is well recognized to be the only one among multiple factors responsible for optic nerve damage in

Table 2. Sequences of primary probes and Invader oligonucleotides

Polymorphism	Location	Base changes	Target	Probe	Sequence
EDN1/T-1370G	5' flanking region	T/G	Anti-sense	T	Flap1-TTGGTGGAGAACAAACAA
				G	Flap2-GTGGTGGAGAACAAACA
				Invader	GGTCTTACTGGGCCACTGTGAGCGCTC
EDN1/+138/ex1 del/ins	Exon 1	del/ins	Sense	A del	Flap1-TAACGGGGAGAAAAGG
				A ins	Flap2-TTAACGGGGAGAAAAGG
				Invader	GCGATCCTTCAGCCCAAGTGCCCTTC
EDN1/G8002A	Intron 4	G/A	Anti-sense	G	Flap1-GAAAATCATTTTGGGGAGC
				A	Flap2-AAAAATCATTTTGGGGAGC
				Invader	TGCCTCTCTGAGTCAATGTATTTACCACTTTCCCTGAGAAATCT
EDN1/K198N	Exon 5	G/T	Sense	G	Flap1-CTTGCCTTTCAGCTTGG
				T	Flap2-ATTGCCTTTCAGCTTGG
				Invader	GTTGTGGGTCACATAACGCTCTCTGGAGGGT
EDNRA/G-231A	Exon 1	G/A	Sense	G	Flap1-CTCCTGGGCACTGC
				A	Flap2-TTCCTGGGCACTGC
				Invader	CTGCACAGCTTCCCCGGCTTCAGAAAACA
EDNRA/H323H	Exon 6	T/C	Anti-sense	T	Flap1-TTTAAGCCGTATATTGAAGAAAA
				C	Flap2-CTTAAGCCGTATATTGAAGAAAA
				Invader	CTTGGTTGTAATTTTTGCTCTTTGCTGGTTCCCTCTTCAA
EDNRA/C+70G	Exon 8	C/G	Sense	C	Flap1-GTCACAGTTGCCTTGT
				G	Flap2-CTCACAGTTGCCTTGT
				Invader	GGAAGAAGGATCAGAGAAGAGATTCCCGGAT
EDNRA/C+1222T	Exon 8	C/T	Anti-sense	C	Flap1-CTTGGGGTTTTCAGTATGA
				T	Flap2-TTTGGGGTTTTCAGTATGA
				Invader	CCCACAAATGCCACCAGAACTTAACGATTCTTCACTTA
EDNRB/L277L	Exon 4	A/G	Anti-sense	A	Flap1-ATTCAGTTTCTATTTCTGCTTG
				G	Flap2-GTTCAGTTTCTATTTCTGCTTG
				Invader	CTCATCCCTATAGTTTTACAAGACAGCAAAAGATTGGTGGCTT

Nine polymorphisms were detected among all participants. These polymorphisms are listed at GeneCanvas. Genotyping of the polymorphisms was performed by the Invader® assay using the probes listed below.

TABLE 3. GENOTYPE AND ALLELE FREQUENCIES

Polymorphism	Sample	Genotype frequency		Chi square p value	Logistic p value	Allele frequency		Chi square p value
		TT	TG+GG			T	G	
EDN1/T-1370G	Control (n=224)	133 (59.4)	91 (40.6)			350 (78.1)	98 (21.9)	
	OAG (n=426)	273 (64.1)	153 (35.9)	0.239	0.561	675 (79.2)	177 (20.8)	0.644
		del/del	del/ins+ ins/ins			del	ins	
EDN1/+138/ex1 del/ins	Control (n=224)	146 (65.2)	78 (34.8)			364 (81.3)	84 (18.8)	
	OAG (n=426)	316 (74.2)	110 (25.8)	0.016	0.206	734 (86.2)	118 (13.8)	0.020
		KK	KN+NN			K	N	
EDN1/K198N	Control (n=224)	98 (43.8)	126 (56.3)			295 (65.8)	153 (34.2)	
	OAG (n=425)	226 (53.2)	199 (46.8)	0.022	0.368	609 (71.6)	241 (28.4)	0.031
		GG	GA+AA			G	A	
EDNRA/G-231A	Control (n=224)	62 (27.7)	162 (72.3)			244 (54.5)	204 (45.5)	
	OAG (n=425)	118 (27.8)	307 (72.2)	0.981	0.777	455 (53.5)	395 (46.5)	0.748
		TT	TC+CC			T	C	
EDNRA/H323H	Control (n=224)	122 (54.5)	102 (45.5)			327 (73.0)	121 (27.0)	
	OAG (n=426)	228 (53.5)	198 (46.5)	0.819	0.539	626 (73.5)	226 (26.5)	0.852
		CC	CG+GG			C	G	
EDNRA/C+70G	Control (n=224)	61 (27.2)	163 (72.8)			229 (51.1)	219 (48.9)	
	OAG (n=426)	128 (30.0)	298 (70.0)	0.453	0.302	462 (54.2)	390 (45.8)	0.286
		CC	CT+TT			C	T	
EDNRA/C+1222T	Control (n=224)	137 (61.2)	87 (38.8)			347 (77.5)	101 (22.5)	
	OAG (n=426)	224 (52.6)	202 (47.4)	0.036	0.122	620 (72.8)	232 (27.2)	0.066
		AA	AG+GG			A	G	
EDNRB/L277L	Control (n=224)	77 (34.4)	147 (65.6)			254 (56.7)	194 (43.3)	
	OAG (n=425)	118 (27.8)	307 (72.2)	0.081	0.096	443 (52.1)	407 (47.9)	0.116

The distributions in controls and OAG patients were consistent with the Hardy-Weinberg equilibrium. Genotype distributions showed no significant differences between OAG patients and control subjects adjusted by age. Data shown are counts with percentages in parentheses. Analysis of the genotype used both a χ^2 test ("Chi square") and logistic regression analysis that allowed adjustment for age ("Logistic p value"); analysis of the allele frequency used a χ^2 test only.

glaucoma. Endothelium derived NO and ET-1 are potent vascular tone modulators important in regulation of local blood flow in the eye [7,35-39].

Furthermore, according to recent studies, ET-1 influences not only blood flow but also morphological and physiological changes relevant to glaucoma. In a rabbit model, optic nerve head ischemia induced by ET-1 resulted in optic disc excavation, diffuse loss of axons, and demyelination affecting the prelaminar portion of the optic nerve without a change in the IOP [40,41]. ET-1 also decreased the anterograde axonal transport in the rat optic nerve [42], caused loss of retinal ganglion cells and their axons in rats [43], and reduced neuronal metabolic activity in the visual cortex of rhesus monkeys [44]. ET-1 induced proliferation in astrocytes cultured from the human optic nerve head by activating ET_A and ET_B receptors [45]. Astrogliosis is a common major pathologic feature shared by many neuropathies, including glaucoma. ET-1 may also affect aqueous humor dynamics in a complex and sometimes self-opposing manner [46-49].

ET_A receptors, the main ET-1 receptor binding sites, are present in the iris, ciliary muscle, ciliary processes, and retina [13,15]. Polak et al. [39] examined the regulation of human retinal blood flow by ET-1, and they concluded that BQ-123, the specific ET_A receptor antagonist, antagonizes the effects of exogenously administered ET-1 on retinal blood flow in healthy subjects. This indicates that the retinal vasoconstrictor effect of ET-1 is mainly mediated via the ET_A receptor. In this study, the genotype distributions adjusted by age showed no significant differences between glaucoma patients and controls. On the other hand, the GG genotype of *EDNRA*/C+70G was associated with more severe visual field defects in NTG patients. This polymorphism did not affect the characteristics of the patients except in NTG patients.

However, the mechanisms by which this polymorphism affects function remain to be determined. Indeed, this polymorphism might be nonfunctional in itself but may be closely linked to a presently uncharacterized functional mutation modifying the expression of the gene. Another possibility might be that the polymorphism is in linkage disequilibrium with another locus, with the causal variant being a small distance away in adjacent regulatory regions or in a nearby gene.

If ET-1 or its receptors are indeed involved in susceptibility to glaucoma, anti-ET-1 therapies are of major interest.

Table 4. Characteristics of glaucoma patients with NTG according to genotype

Polymorphism	Characteristic	Genotype CC+GG	Genotype GG	Mann-Whitney p value	Logistic regression p value
EDNRA/C+70G	Age at diagnosis (years)	55.7±13.3 (n=194)	57.8±12.7 (n=54)	0.379	0.306
	Untreated maximum IOP (mm Hg)	17.0±2.2 (n=189)	16.5±2.3 (n=53)	0.141	0.105
	Visual field score at diagnosis	2.7±0.7 (n=195)	3.0±0.7 (n=55)	0.014	0.027

The GG genotype of *EDNRA*/C+70G was associated with worse visual field defects in NTG patients (p=0.014, Mann-Whitney U test; p=0.027, logistic regression analysis). Data shown are expressed as means±standard deviation.

Because ET-1 may participate in vascular dysfunction such as vasoconstriction or abnormal autoregulation in glaucoma, an ET-1 blocker or ET-1 receptor antagonist might be of some benefit in glaucoma patients, especially those NTG patients whose glaucoma etiology appears to be vascular insufficiency. For example, isopropyl unoprostone (Rescula®), already used to lower IOP in some glaucoma patients, has been reported to have anti-ET-1 effects in animals and in healthy human subjects [50-52].

In conclusion, our results suggest that the polymorphism of *EDNRA*/C+70G may be related to NTG risk factors. Glaucoma is caused by actions of many genes, each having a small additive effect, interacting with effects of the environment. Actions of ET-1 and its receptors could be among contributing influences. However, given insufficient present knowledge of the functional mechanisms involving this polymorphism, such findings cannot explain the pathogenesis of glaucoma at this time. Further studies are necessary to assess the functional impact of these polymorphisms on gene expression or structure.

ACKNOWLEDGEMENTS

This study was supported by Research on Eye and Ear Sciences from Ministry of Health, Labour and Welfare of Japan.

REFERENCES

1. Quigley HA. Number of people with glaucoma worldwide. Br J Ophthalmol 1996; 80:389-93.
2. Quigley HA. Open-angle glaucoma. N Engl J Med 1993; 328:1097-106.
3. Iwase A, Suzuki Y, Araie M, Yamamoto T, Abe H, Shirato S, Kuwayama Y, Mishima HK, Shimizu H, Tomita G, Inoue Y, Kitazawa Y, Tajimi Study Group, Japan Glaucoma Society. The prevalence of primary open-angle glaucoma in Japanese: the Tajimi Study. Ophthalmology 2004; 111:1641-8.
4. Teikari JM. Genetic influences in open-angle glaucoma. Int Ophthalmol Clin 1990; 30:161-8.
5. Yablonski ME. An analysis of the "vascular hypothesis" concerning optic disc pathology in glaucoma. Ann Ophthalmol 1979; 11:67-9.
6. Yorio T, Krishnamoorthy R, Prasanna G. Endothelin: is it a contributor to glaucoma pathophysiology? J Glaucoma 2002; 11:259-70.
7. Haefliger IO, Dettmann E, Liu R, Meyer P, Prunte C, Messerli J, Flammer J. Potential role of nitric oxide and endothelin in the pathogenesis of glaucoma. Surv Ophthalmol 1999; 43 Suppl 1:S51-8.
8. Yanagisawa M, Kurihara H, Kimura S, Tomobe Y, Kobayashi M, Mitsui Y, Yazaki Y, Goto K, Masaki T. A novel potent vasoconstrictor peptide produced by vascular endothelial cells. Nature 1988; 332:411-5.
9. Inoue A, Yanagisawa M, Kimura S, Kasuya Y, Miyauchi T, Goto K, Masaki T. The human endothelin family: three structurally and pharmacologically distinct isopeptides predicted by three separate genes. Proc Natl Acad Sci U S A 1989; 86:2863-7.
10. Vane J. Endothelins come home to roost. Nature 1990; 348:673.
11. Arai H, Hori S, Aramori I, Ohkubo H, Nakanishi S. Cloning and expression of a cDNA encoding an endothelin receptor. Nature 1990; 348:730-2.

12. Sakurai T, Yanagisawa M, Takuwa Y, Miyazaki H, Kimura S, Goto K, Masaki T. Cloning of a cDNA encoding a non-isopeptide-selective subtype of the endothelin receptor. Nature 1990; 348:732-5.
13. Fernandez-Durango R, Rollin R, Mediero A. Roldan-Pallares M, Garcia Feijo J, Garcia Sanchez J, Fernandez-Cruz A, Ripodas A. Localization of endothelin-1 mRNA expression and immunoreactivity in the anterior segment of human eye: expression of ETA and ETB receptors. Mol Vis 2003; 9:103-9.
14. Lepple-Wienhues A, Becker M, Stahl F, Berweck S, Hensen J, Noske W, Eichhorn M, Wiederholt M. Endothelin-like immunoreactivity in the aqueous humour and in conditioned medium from cultured ciliary epithelial cells. Curr Eye Res 1992; 11:1041-6.
15. Ripodas A, de Juan JA, Roldan-Pallares M, Bernal R, Moya J, Chao M, Lopez A, Fernandez-Cruz A, Fernandez-Durango R. Localisation of endothelin-1 mRNA expression and immunoreactivity in the retina and optic nerve from human and porcine eye. Evidence for endothelin-1 expression in astrocytes. Brain Res 2001; 912:137-43.
16. Narayan S, Brun AM, Yorio T. Endothelin-1 distribution and basolateral secretion in the retinal pigment epithelium. Exp Eye Res 2004; 79:11-9.
17. Prasanna G, Dibas A, Tao W, White K, Yorio T. Regulation of endothelin-1 in human non-pigmented ciliary epithelial cells by tumor necrosis factor-alpha. Exp Eye Res 1998; 66:9-18.
18. Noske W, Hensen J, Wiederholt M. Endothelin-like immunoreactivity in aqueous humor of patients with primary open-angle glaucoma and cataract. Graefes Arch Clin Exp Ophthalmol 1997; 235:551-2.
19. Tezel G, Kass MA, Kolker AE, Becker B, Wax MB. Plasma and aqueous humor endothelin levels in primary open-angle glaucoma. J Glaucoma 1997; 6:83-9.
20. Kallberg ME, Brooks DE, Garcia-Sanchez GA, Komaromy AM, Szabo NJ, Tian L. Endothelin 1 levels in the aqueous humor of dogs with glaucoma. J Glaucoma 2002; 11:105-9.
21. Sugiyama T, Moriya S, Oku H, Azuma I. Association of endothelin-1 with normal tension glaucoma: clinical and fundamental studies. Surv Ophthalmol 1995; 39 Suppl 1:S49-56.
22. Cellini M, Possati GL, Profazio V, Sbrocca M, Caramazza N, Caramazza R. Color Doppler imaging and plasma levels of endothelin-1 in low-tension glaucoma. Acta Ophthalmol Scand Suppl 1997; 224:11-3.
23. Kaiser HJ, Flammer J, Wenk M, Luscher T. Endothelin-1 plasma levels in normal-tension glaucoma: abnormal response to postural changes. Graefes Arch Clin Exp Ophthalmol 1995; 233:484-8.
24. Nicolela MT, Ferrier SN, Morrison CA, Archibald ML, LeVatte TL, Wallace K, Chauhan BC, LeBlanc RP. Effects of cold-induced vasospasm in glaucoma: the role of endothelin-1. Invest Ophthalmol Vis Sci 2003; 44:2565-72.
25. Buckley C, Hadoke PW, Henry E, O'Brien C. Systemic vascular endothelial cell dysfunction in normal pressure glaucoma. Br J Ophthalmol 2002; 86:227-32.
26. Gass A, Flammer J, Linder L, Romerio SC, Gasser P, Haefeli WE. Inverse correlation between endothelin-1-induced peripheral microvascular vasoconstriction and blood pressure in glaucoma patients. Graefes Arch Clin Exp Ophthalmol 1997; 235:634-8.
27. Tunny TJ, Richardson KA, Clark CV. Association study of the 5' flanking regions of endothelial-nitric oxide synthase and endothelin-1 genes in familial primary open-angle glaucoma. Clin Exp Pharmacol Physiol 1998; 25:26-9.
28. Brezin AP, Bechetoille A, Hamard P, Valtot F, Berkani M, Belmouden A, Adam MF, Dupont de Dinechin S, Bach JF, Garchon HJ. Genetic heterogeneity of primary open angle glaucoma and ocular hypertension: linkage to GLC1A associated with an increased risk of severe glaucomatous optic neuropathy. J Med Genet 1997; 34:546-52.
29. Copin B, Brezin AP, Valtot F, Dascotte JC, Bechetoille A, Garchon HJ. Apolipoprotein E-promoter single-nucleotide polymorphisms affect the phenotype of primary open-angle glaucoma and demonstrate interaction with the myocilin gene. Am J Hum Genet 2002; 70:1575-81.
30. Kosaki H, Inoue Y. [A new classification of stages of chronic glaucomas]. Nippon Ganka Gakkai Zasshi 1972; 76:1258-67.
31. Hosoda M, Hirano T, Tsukahara S. [Mode of progression of visual field defects and risk factors in glaucoma patients]. Nippon Ganka Gakkai Zasshi 1997; 101:593-7.
32. Anderson DR, Patella VM. Automated Static Perimetry. 2nd Ed. St. Louis, MO: Mosby; 1999. p. 121-190.
33. Lyamichev V, Mast AL, Hall JG, Prudent JR, Kaiser MW, Takova T, Kwiatkowski RW, Sander TJ, de Arruda M, Arco DA, Neri BP, Brow MA. Polymorphism identification and quantitative detection of genomic DNA by invasive cleavage of oligonucleotide probes. Nat Biotechnol 1999; 17:292-6.
34. Drance SM, Sweeney VP, Morgan RW, Feldman F. Studies of factors involved in the production of low tension glaucoma. Arch Ophthalmol 1973; 89:457-65.
35. Haefliger IO, Flammer J, Luscher TF. Nitric oxide and endothelin-1 are important regulators of human ophthalmic artery. Invest Ophthalmol Vis Sci 1992; 33:2340-3.
36. Orgul S, Cioffi GA, Bacon DR, Van Buskirk EM. An endothelin-1-induced model of chronic optic nerve ischemia in rhesus monkeys. J Glaucoma 1996; 5:135-8.
37. Meyer P, Flammer J, Luscher TF. Endothelium-dependent regulation of the ophthalmic microcirculation in the perfused porcine eye: role of nitric oxide and endothelins. Invest Ophthalmol Vis Sci 1993; 34:3614-21.
38. Schmetterer L, Findl O, Strenn K, Jilma B, Graselli U, Eichler HG, Wolzt M. Effects of endothelin-1 (ET-1) on ocular hemodynamics. Curr Eye Res 1997; 16:687-92.
39. Polak K, Luksch A, Frank B, Jandrasits K, Polska E, Schmetterer L. Regulation of human retinal blood flow by endothelin-1. Exp Eye Res 2003; 76:633-40.
40. Cioffi GA, Sullivan P. The effect of chronic ischemia on the primate optic nerve. Eur J Ophthalmol 1999; 9 Suppl 1:S34-6.
41. Oku H, Sugiyama T, Kojima S, Watanabe T, Azuma I. Experimental optic cup enlargement caused by endothelin-1-induced chronic optic nerve head ischemia. Surv Ophthalmol 1999; 44 Suppl 1:S74-84.
42. Stokely ME, Brady ST, Yorio T. Effects of endothelin-1 on components of anterograde axonal transport in optic nerve. Invest Ophthalmol Vis Sci 2002; 43:3223-30.
43. Chauhan BC, LeVatte TL, Jollimore CA, Yu PK, Reitsamer HA, Kelly ME, Yu DY, Tremblay F, Archibald ML. Model of endothelin-1-induced chronic optic neuropathy in rat. Invest Ophthalmol Vis Sci 2004; 45:144-52.
44. Brooks DE, Kallberg ME, Cannon RL, Komaromy AM, Ollivier FJ, Malakhova OE, Dawson WW, Sherwood MB, Kuekuerichkina EE, Lambrou GN. Functional and structural analysis of the visual system in the rhesus monkey model of optic nerve head ischemia. Invest Ophthalmol Vis Sci 2004; 45:1830-40.
45. Prasanna G, Krishnamoorthy R, Clark AF, Wordinger RJ, Yorio T. Human optic nerve head astrocytes as a target for endothelin-

1. Invest Ophthalmol Vis Sci 2002; 43:2704-13.
46. Lepple-Wienhues A, Stahl F, Willner U, Schafer R, Wiederholt M. Endothelin-evoked contractions in bovine ciliary muscle and trabecular meshwork: interaction with calcium, nifedipine and nickel. Curr Eye Res 1991; 10:983-9.
47. Wiederholt M, Bielka S, Schweig F, Lutjen-Drecoll E, Lepple-Wienhues A. Regulation of outflow rate and resistance in the perfused anterior segment of the bovine eye. Exp Eye Res 1995; 61:223-34.
48. Erickson-Lamy K, Korbmacher C, Schuman JS, Nathanson JA. Effect of endothelin on outflow facility and accommodation in the monkey eye in vivo. Invest Ophthalmol Vis Sci 1991; 32:492-5.
49. Prasanna G, Dibas A, Hulet C, Yorio T. Inhibition of Na(+)/K(+)-atpase by endothelin-1 in human nonpigmented ciliary epithelial cells. J Pharmacol Exp Ther 2001; 296:966-71.
50. Sugiyama T, Azuma I. Effect of UF-021 on optic nerve head circulation in rabbits. Jpn J Ophthalmol 1995; 39:124-9.
51. Yu DY, Su EN, Cringle SJ, Schoch C, Percicot CP, Lambrou GN. Comparison of the vasoactive effects of the docosanoid unoprostone and selected prostanoids on isolated perfused retinal arterioles. Invest Ophthalmol Vis Sci 2001; 42:1499-504.
52. Polska E, Doelemeyer A, Luksch A, Ehrlich P, Kaehler N, Percicot CL, Lambrou GN, Schmetterer L. Partial antagonism of endothelin 1-induced vasoconstriction in the human choroid by topical unoprostone isopropyl. Arch Ophthalmol 2002; 120:348-52.

The print version of this article was created on 23 Jun 2005. This reflects all typographical corrections and errata to the article through that date. Details of any changes may be found in the online version of the article.

Lactoferrin Glu561Asp facilitates secondary amyloidosis in the cornea

K Araki-Sasaki, Y Ando, M Nakamura, K Kitagawa, S Ikemizu, T Kawaji, T Yamashita, M Ueda, K Hirano, M Yamada, K Matsumoto, S Kinoshita and H Tanihara

Br. J. Ophthalmol. 2005;89;684-688
doi:10.1136/bjo.2004.056804

EXTENDED REPORT

Lactoferrin Glu561Asp facilitates secondary amyloidosis in the cornea

K Araki-Sasaki, Y Ando, M Nakamura, K Kitagawa, S Ikemizu, T Kawaji, T Yamashita, M Ueda, K Hirano, M Yamada, K Matsumoto, S Kinoshita, H Tanihara

Br J Ophthalmol 2005;**89**:684–688. doi: 10.1136/bjo.2004.056804

See end of article for authors' affiliations

Correspondence to: Yukio Ando, MD, PhD, Department of Diagnostic Medicine, Graduate School of Medical Sciences, Kumamoto University, 1-1-1 Honjo, Kumamoto 860-0811, Japan; yukio@kaiju.medic.kumamoto-u.ac.jp

Accepted for publication 5 October 2004

Aim: To elucidate the pathogenic mechanism of amyloid formation in corneal amyloidosis with trichiasis.
Methods: Ophthalmological examination was performed in nine patients to determine secondary corneal amyloidosis with trichiasis. Congo red staining and immunohistochemistry using anti-human lactoferrin antibody were used for biopsied corneal samples. For genetic analyses, single strand conformation polymorphism (SSCP), direct DNA sequence analysis, and polymerase chain reaction (PCR) induced mutation restriction analysis (IMRA) were employed to detect lactoferrin gene polymorphism.
Results: All patients had had trichiasis at least for 1 year, and all amyloid-like deposits were found in one eye with trichiasis. Ophthalmological examination revealed that eight patients showed gelatinous type of amyloid deposition and one showed lattice type of amyloid deposition. Studies of biopsied corneal samples with Congo red stain revealed positive staining just under the corneal epithelial cells. Immunoreactivity of anti-human lactoferrin antibodies was recognised in all tissues with positive Congo red staining. Lactoferrin gene analysis revealed that seven patients were heterozygotic and two were homozygotic for lactoferrin Glu561Asp. The frequency of the polymorphism in the patients was significantly different from that in 56 healthy control subjects.
Conclusion: Lactoferrin Glu561Asp is a key polymorphism related to facilitating amyloid formation in corneal amyloidosis with trichiasis.

Amyloidosis is a disorder of protein metabolism in which normally soluble autologous proteins are deposited in tissues as abnormal insoluble fibrils, which cause structural and functional disruptions.[1 2] Thus far, 24 different precursor proteins of amyloid fibrils have been identified in systemic and localised amyloidoses.[3] Of these precursors, the mutated proteins, with conformations different from those of wild type proteins, often become amyloidogenic proteins.[4–6]

Ocular tissue is one type of tissue in which several different types of amyloid precursor proteins deposit as amyloid fibrils.[7 8] Most of the precursors that occur in ocular tissues in systemic amyloidosis have been identified.[9–14] Secondary corneal amyloidosis has been reported to occur in cases of keratoconus, trachoma, phlyctenular keratitis, bullous keratopathy, interstitial keratitis, syphilis, and trichiasis. Although amyloid deposits, with possible co-localisation of several proteins, have been observed,[14 15] the precursor protein of the amyloid remained to be unidentified. We previously reported that the precursor protein in corneal amyloidosis associated with trichiasis is lactoferrin.[16] Although all of the patients in the previous study were heterozygotes for lactoferrin Glu561Asp gene, no statistical significance was observed when compared with that of the polymorphism in healthy control subjects. Although trichiasis itself is not so uncommon, the incidence of corneal amyloidosis is quite low.[10 17] Some additional factor or factors, such as polymorphism in lactoferrin gene, may thus be involved in corneal amyloidosis with trichiasis.

Because we recently encountered an additional six patients with corneal amyloidosis with trichiasis, we examined the relation between the lactoferrin gene polymorphism and corneal amyloidosis.

PATIENTS AND METHODS

Patients

The patients' profiles are presented in table 1. Neurological examination and blood analysis indicated no signs of systemic amyloidosis, and no amyloid deposition was found by Congo red staining of a biopsy specimen of the gastric and duodenal mucosae. After informed consent, the corneal regions of patient 1–5, and 8 and the cilia of patient 9 were excised and subjected to histological examination. The study was approved by the ethics committee of Graduate School of Medical Sciences, Kumamoto University.

Materials

Polyclonal anti-human lactoferrin antibody and other antibodies, such as polyclonal anti-human transthyretin, anti-human kappa, lambda light chain, anti-human lysozyme antibodies, and monoclonal anti-human AA and anti-human keratin antibodies were purchased from Sigma Chemical Co (St Louis, MO, USA) and Dako Corp (Carpinteria, CA, USA), respectively. Chemicals used in histochemical and biochemical studies were of analytical grade.

Congo red staining

For all specimens, formalin fixed, paraffin embedded sections were stained with haematoxylin and eosin and Congo red and were examined under polarised light for the presence of green birefringence.

Immunohistochemical analysis of biopsy specimens

Specimens were fixed in 4% buffered paraformaldehyde. Paraffin embedded biopsy samples were serially cut at 4 μm. To detect the immunoreactivity for antibodies in amyloid deposits, the ABC method was used (Dako, Glostrup, Denmark) according to the manufacturer's instructions.

Abbreviations: IMRA, induced mutation restriction analysis; PCR, polymerase chain reaction; SSCP, single strand conformation polymorphism

Table 1 Patient profile

Patient No	Age (year)	Sex	Lesion	Duration of disorder (years)	Histopathology	Genotype
1	30	M	Right downward	3	+	Hetero
2	41	F	Right downward	16	+	Hetero
3	67	F	Right downward	10	+	Hetero
4	17	F	Right downward	4–5	+	Hetero
5	62	F	Right downward	3	+	Homo
6	12	F	Right downward	1<	np	Hetero
7	78	F	Right downward	10	np	Hetero
8	17	F	Left downward	17	+	Hetero
9	85	M	Right downward	1–2	np	Homo

Hetero, heterozygotic for the lactoferrin Glu561Asp gene; Homo, homozygotic for the lactoferrin Glu561Asp gene. np: not performed. 1<: more than 1 year.

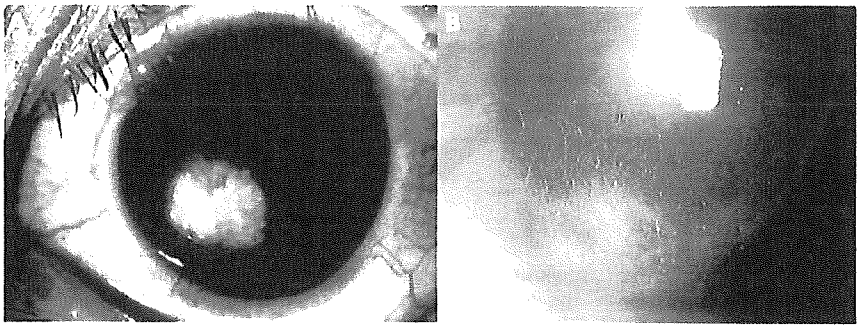

Figure 1 Amyloid deposits in the cornea of patients 1 (A) and 9 (B).

DNA isolation

In patients 1 and 4–9 in table 1, total genomic DNA was isolated from peripheral blood cells as described previously.[18] In patients 2 and 3, total genomic DNA was isolated from paraffin sections by using the Depat kit (Takara Co, Shiga, Japan).

Single strand conformation polymorphism (SSCP) analysis

SSCP analysis was performed according to the method of Orita *et al.*[19] The polymerase chain reaction (PCR) primer sets used based on previous reports[20] (GenBank Database accession no U95626) was described in table 2.

Direct DNA sequence analysis

The PCR products (5 ng) of exons 2, 9, 10, and 15 from the patient and the control subjects were analysed, using 5′ and 3′ primers, by Thermo Sequenase radiolabelled terminator cycle sequencing kit (Amersham, Uppsala, Sweden).

PCR induced mutation restriction analysis (IMRA)

To confirm the polymorphism Ala11Thr, PCR was performed with the exon 2 primer set, and then PCR products were digested with ApaLI. To confirm the other polymorphism (Glu561Asp), we prepared the Glu561Asp PCR-IMRA primer (5′-GTCTGCCAGCTTCA AATCCTTAGC CCAGAC-3′), which annealed immediately 3′ to the polymorphism and contained mismatch bases (GA instead of a normal TG at the 2′, 3′ position from the 3′ end) that created a unique *Aat*II restriction site, only when the lactoferrin gene had a C at position 3 of codon 561. After PCR amplification using the Glu561Asp PCR-IMRA primer and exon 15 outer primer (5′-GAAGCTCCTTCTCTGTTCCTCACA-3′), PCR products were digested with *Aat*II. After informed consent was obtained,

Table 2 Primer sets used in this study

Exon	Upstream primer	Downstream primer
1	5′-CCAGCCGAGTTTCTCAAGTC-3′	5′-CCCCAGGCACCTGCACTCAC-3′
2	5′-CCTTGGCCCCTCTCTCCCAG-3′	5′-AACACCCGGCATTGACTCAC-3′
3	5′-TCTGGCCTCTTTACTTTCAG-3′	5′-GGGTCCCCAGGCAGAACTAC-3′
4	5′-TTCTGTCTGCCCCTTTGCAG-3′	5′-TATGCCCCCAGCCATCTTAC-3′
5	5′-CACTTCTCTGTGTTTAACAG-3′	5′-AAGGGGACAGGGTCACTCAC-3′
6	5′-GATGGTTTCTCTTTTCACAG-3′	5′-GCTCATTACCCTGCTCTTAC-3′
7	5′-CCACCTCACCTTCCCTGCAG-3′	5′-AAGTGGGGAGGACCGTGGGT-3′
8	5′-TCCCTATTTACCATTGACAC-3′	5′-AAGTAGAAGACCACACCAGG-3′
9	5′-GCAAAGCTCAGGTTGCCCAG-3′	5′-ATGCCCAGGCCCTAGGTCTT-3′
10	5′-AGCCTCACTGTGGTGCTGGA-3′	5′-ACTCCCATGACCCAGAGGGA-3′
11	5′-AGAGTTTGTGGCTTCTCACT-3′	5′-CCAGCAACAAGAACTTATCC-3′
12	5′-CCTGGAGGTTAAGACTTGTT-3′	5′-CCACAGCACAATATGCCTAC-3′
13	5′-TGGACTCAGGTTTGAAGAGC-3′	5′-GCTGAGGGATGAGGTAAGTC-3′
14	5′-GAAAGCCCCACTAGTTTCTC-3′	5′-CCAAAGACTCTGCTTTGAAG-3′
15	5′-CGTGGATGATGCCACCTTCT-3′	5′-GCCCACACAGCTAAGAAAGC-3′
16	5′-CTTAGCTACTCACTGTCTGC-3′	5′-CTTCACCCATGGTGGTTTCT-3′
17	5′-GTTTCTGAATCTCTTGCTCT-3′	5′-AGAGCAGGGAATTGTAAGCA-3′

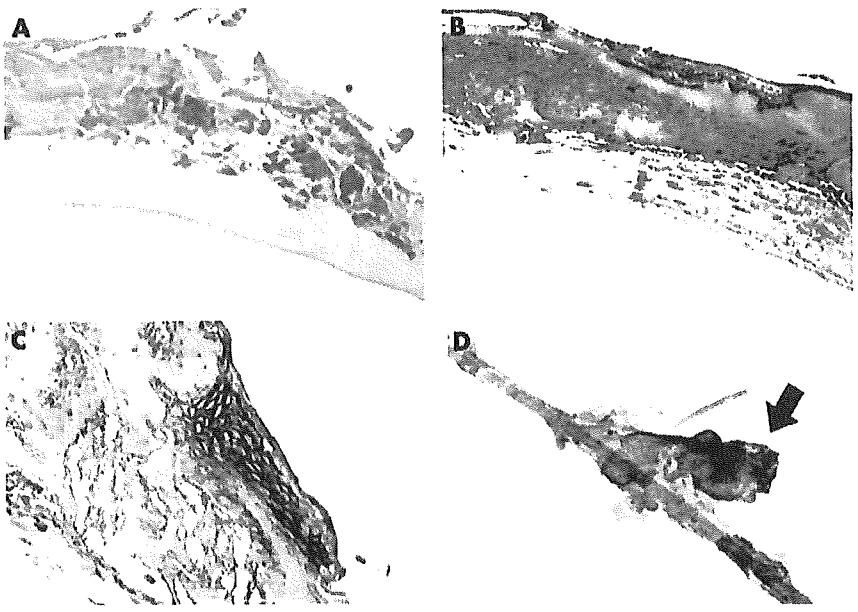

Figure 2 Histochemical analysis for the excised cornea, (A) and (B) Congo red staining and an anti-human lactoferrin antibody staining of the sample from patient 8. (C) An anti-human lactoferrin antibody staining of the corneal epithelium of patient 8. (D) Immunohistochemistry using an anti-human lactoferrin antibody for cilia in patient 9. The arrow indicates the positive stained mass stuck on the cilia. Magnification ×100.

56 healthy Japanese volunteers were also examined in the same way to determine the frequency of these polymorphisms.

Statistical analysis

Frequency of lactoferrin Glu561Asp gene was compared in control subjects and the patients using Fisher's exact test. p Values less than 0.05 were considered significant.

RESULTS

Macroscopic examination

Eight patients showed gelatinous type of amyloid deposition (fig 1A), and one showed lattice type of amyloid deposition (fig 1B). All patients had had trichiasis at least for 1 year (table 1), and all amyloid-like deposits were found in one eye with trichiasis.

Histochemical analyses of biopsied corneal samples

Congo red staining for biopsied corneal samples in patient 1–5 and 8 revealed positive staining just under the corneal epithelial cells that extended into the stroma (fig 2A). No vascularisation was observed. Immunoreactivity of anti-human lactoferrin antibodies was recognised in all tissues with positive Congo red staining (fig 2B). Notably, extracellular space of the corneal epithelial cells was clearly stained with an anti-lactoferrin antibody (fig 2C). Other antibodies showed no immunoreactivity for the amyloid deposits. Specificity controls were obtained by preincubating the anti-human lactoferrin antibody with lactoferrin (1–10 μg/ml).[21]

Although we could not perform a biopsy on patient 9 for ethical reasons, a lactoferrin positive material stuck on the excised cilia (fig 2D).

Analyses of the lactoferrin gene

SSCP analyses for DNA from a 30 year old male patient (No 1) revealed abnormally migrating bands in exons 2, 9, 10, and 15. Direct sequencing using exons 2, 9, 10, and 15 PCR products from the patients' DNA was performed to identify these polymorphisms. In exons 9 and 10, two polymorphisms were detected (data not shown): a GTC (Val) to GTT (Val) substitution in codon 346 of exon 9 and a GGA (Gly) to GGG (Gly) substitution in codon 398 of exon 10. In exons 2 and 15, two polymorphisms were detected: amino acid substitutions at codon 11 from GCC (Ala) to ACC (Thr) and at codon 561 from GAG (Glu) to GAC (Asp) (data not shown). Since the conversion of amino acid was observed in lactoferrin Ala11Thr and Glu561Asp, PCR-IMRA was performed in other patients to examine these polymorphisms.

Analysis via PCR-IMRA revealed that seven of nine patients were heterozygotic and two homozygotic for lactoferrin Glu561Asp (fig 3). Although one patient was heterozygotic for lactoferrin Ala11Thr, other patients showed no such polymorphism. We also used genetic analysis to

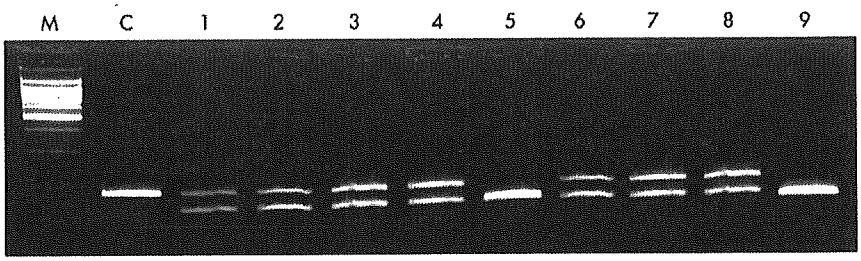

Figure 3 Detection of the lactoferrin Glu561Asp gene by means of PCR-IMRA, M represents the 100 bp DNA size marker; C represents the data from control subject; Numbers 1–9 correspond the patient numbers given in table 1. Analyses for lactoferrin Glu561Asp were performed via PCR-IMRA as described.[16] When allele for lactoferrin Glu561Asp only exists, the digestion bands (158 bp and 28 bp) are observed.

Table 3 Frequency of the lactoferrin genotype in healthy volunteers

	Lactoferrin Glu561Asp	Number of subjects	Frequency of genotype (%)
No polymorphism	−/−	31	56.3
Heterozygote	+/−	18	32.7
Homozygote	+/+	7	12.7

determine the frequency of the lactoferrin Glu561Asp gene in 56 healthy Japanese volunteers. Comparison of this frequency in healthy volunteers with the frequency in patients revealed significant polymorphism in the patients (Fisher's exact test = 0.0119, $p<0.01$)(table 3).

DISCUSSION

We suggested in this study that lactoferrin Glu561Asp facilitates amyloid formation in corneal amyloidosis with trichiasis. We speculate that lactoferrin from tears should be a source of amyloid formation in the cornea of patients for the following four reasons. Firstly, lactoferrin is the major component of tears. Secondly, anti-human lactoferrin antibody reactive mass stuck to cilia (fig 2D). Thirdly, lactoferrin was clearly detected in the intracellular space of the corneal epithelium. And fourthly, lactoferrin was observed in amyloid deposits in all samples examined (fig 2). Although we cannot deny the possibility that continuous stimulation by trichiasis may induce corneal epithelial cells and stromal fibroblasts to secrete the amyloidogenic protein, because these cells have the potential producing amyloid protein in certain situations,[22] we conclude that mutated lactoferrin derived from tears might infiltrate into the site of amyloid deposition through the extracellular space of the epithelial cells. We also performed the lactoferrin gene analysis and histochemistry of three samples of corneal amyloidosis with keratoconus. Although anti-lactoferrin antibody showed a positive reaction, no polymorphism in the lactoferrin gene was detected (data not shown). In this type of amyloidosis, the parenchyma already has abnormal structures that may show an affinity with native lactoferrin. But, in corneal amyloidosis with trichiasis, the polymorphism may be an indispensable factor because the parenchyma, the targeted lesion of amyloid deposition, has normal structures.

We carefully checked the pattern of anti-lactoferrin antibody reactivity of lactoferrin Glu561Asp gene in the heterozygotic and homogygotic patients. However, no obvious difference was detected. This may be because the degree of the amyloidotic changes in the corneal may be too immature to be compared. Accumulation of such cases for comparison is needed.

We previously reported that lactoferrin forms an amyloid mass both in in vitro examination and in the cornea.[16] However, the relation between lactoferrin gene polymorphisms and the amyloid formation mechanism remained to be elucidated because statistical differences in the frequency of the polymorphism between the patients and control subjects was not clear.

To investigate whether the mutated form of lactoferrin has amyloidogenic ability, a possible conformational change of the protein was simulated. According to the PDB code (www.rcsb.org/), the amino acid at position 561 in lactoferrin locates in a loop region at the bottom of the C-lobe (fig 4A). This loop region has relatively high B factors, which indicates this region's flexibility.[23] Oxygen of the Glu561 side chain forms a weak hydrogen bond with the side chain's nitrogen atom of Trp563 at a distance of 3.32 Å (fig 4B). The polymorphism of Glu561Asp in lactoferrin seems to have no hydrogen bond or has a weaker interaction with Trp563. This might enhance flexibility of this loop region, and then

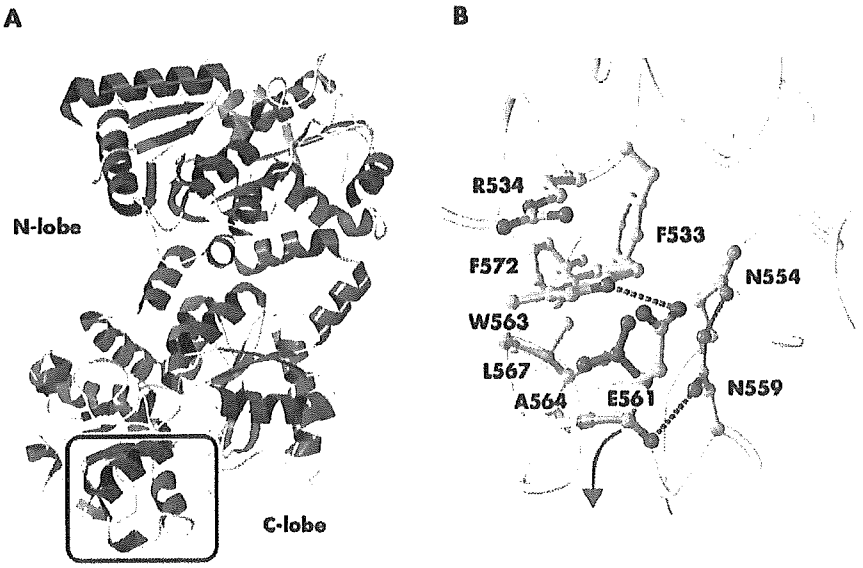

Figure 4 Structural feature of the human lactoferrin Glu561. (A) A ribbon diagram of human lactoferrin. The region depicted in close up (B) is indicated by a rectangle. (B) The main chain backbone is shown in grey. The residues, which involve the charged or hydrophobic interaction network in this region, are shown as a ball and stick model. The Asp mutated from Glu561 is shown in purple.

expose the hydrophobic patch. Consequently, the mutant lactoferrin may form amyloid fibrils via this exposed hydrophobic patch.

Clinically, our nine patients showed the two different types of amyloidosis. It is well known that hereditary corneal amyloidosis has been classified into two types, gelatinous and lattice,[24] with a pathogenesis related to mutated M1S1[25 26] and TGFBI[27] genes, respectively. Majima *et al* speculated that amyloid deposition in the corneal stroma resulted in a lattice pattern and deposition in the epithelium resulted in a gelatinous pattern (personal communication). From our patients' clinical observations, we derive the following: in gelatinous-type secondary corneal amyloidosis, lactoferrin aggregates into the epithelial layer through the extracellular space of the epithelium where cilia repeatedly touch. In contrast, in lattice-type secondary corneal amyloidosis, epithelial erosion with destruction of Bowman's membrane might enable lactoferrin to integrate into the stroma and form amyloid deposition.

From our study, we conclude that secondary corneal amyloidosis with trichiasis is predominantly induced by both trichiasis and lactoferrin Glu561Asp polymorphism.

ACKNOWLEDGEMENTS

This work was supported by grants from the Amyloidosis Research Committee, the Pathogenesis, Therapy of Hereditary Neuropathy Research Committee, the Surveys and Research on Specific Disease, the Ministry of Health and Welfare of Japan, Charitable Trust Clinical Pathology Research Foundation of Japan, and Research for the Future Program Grant, and Grants in Aid for Scientific Research (B) 15390275 and (B) 20253742 from the Ministry of Education, Science, Sports and Culture of Japan. The authors thank Hiroko Katsura, and Miyo Okajima for technical assistance.

Authors' affiliations

K Araki-Sasaki, T Kawaji, K Matsumoto, H Tanihara, Department of Ophthalmology, Graduate School of Medical Sciences, Kumamoto University, 1-1-1 Honjo, Kumamoto 860-0811, Japan
Y Ando, M Nakamura, Department of Diagnostic Medicine, Graduate School of Medical Sciences, Kumamoto University, 1-1-1 Honjo, Kumamoto 860-0811, Japan
K Kitagawa, Department of Ophthalmology, Kanazawa Medical University Hospital, 1-1 Daigaku, Uchinada-machi, Kahoku-gun, Ishikawa 920-0293, Japan
S Ikemizu, Department of Structural Biology, Graduate School of Medical Sciences, Kumamoto University, 1-1-1 Honjo, Kumamoto 860-0811, Japan
T Yamashita, M Ueda, Department of Neurology, Graduate School of Medical Sciences, Kumamoto University, 1-1-1 Honjo, Kumamoto 860-0811, Japan
K Hirano, Department of Ophthalmology, Japanese Red Cross Nagoya First Hospital, 3-35 Michishita-cho, Nagoya 453-8511, Japan
M Yamada, Division for Vision Research, National Institute of Sensory Organs, National Tokyo Medical Center, 2-5-1 Higashigaoka, Meguro 152-8902, Tokyo, Japan
S Kinoshita, Department of Ophthalmology, Kyoto Prefectural University of Medicine, 465 Kajii-cho, Kawaramachidori Noboru, Kamigyoku, Kyoto 602-8566, Japan

Competing interests: The authors have no proprietary, financial, or commercial interests in any of the companies or products mentioned in this paper.

REFERENCES

1 **Glenner GG,** Page DL. Amyloid, amyloidosis, and amyloidogenesis. *Int Rev Exp Pathol* 1976;**15**:1–92.
2 **Tan SY,** Pepys MB. Amyloidosis. *Histopathology* 1994;**25**:403–14.
3 **Westermark P,** Benson MD, Buxbaum JN, *et al.* Amyloid fibril protein nomenclature—2002. *Amyloid* 2002;**9**:197–200.
4 **Gorevic PD,** Munoz PC, Gorgone G, *et al.* Amyloidosis due to a mutation of the gelsolin gene in an American family with lattice corneal dystrophy type II. *N Engl J Med* 1991;**325**:1780–5.
5 **Colon W,** Lai Z, McCutchen SL, *et al.* FAP mutations destabilize transthyretin facilitating conformational changes required for amyloid formation. *Ciba Found Symp* 1996;**199**:228–38.
6 **Goldsteins G,** Persson H, Andersson K, *et al.* Exposure of cryptic epitopes on transthyretin only in amyloid and in amyloidogenic mutants. *Proc Natl Acad Sci USA* 1999;**96**:3108–13.
7 **Sandgren O.** Ocular amyloidosis. with special reference to the hereditary forms with vitreous involvement. *Surv Ophthalmol* 1995;**40**:173–96.
8 **Ando E,** Ando Y, Okamura R, *et al.* Ocular manifestation of familial amyloidotic polyneuropathy type I: long term follow up. *Br J Ophthalmol* 1997;**81**:295–8.
9 **Rodrigues M,** Zimmerman LE. Secondary amyloidosis in ocular leprosy. *Arch Ophthalmol* 1971;**85**:277–9.
10 **Hayasaka S,** Setogawa T, Ohmura M. Secondary localized amyloidosis of the cornea caused by trichiasis. *Ophthalmologica* 1987;**194**:77–81.
11 **Watts J,** Frank H. Corneal amyloidosis. *Br J Ophthalmol* 1989;**73**:674–6.
12 **Hill JC,** Maske R, Bowen RM. Secondary localized amyloidosis of the cornea associated with tertiary syphilis. *Cornea* 1990;**9**:98–101.
13 **Dutt S,** Elner VM, Soong HK, *et al.* Secondary localized amyloidosis in interstitial keratitis. Clinicopathologic findings. *Ophthalmology* 1992;**99**:817–23.
14 **Aso K,** Wakakura M. Corneal amyloidosis complicated by trichiasis. Immunohistochemical identification of the amyloid light chain protein. *Jpn J Ophthalmol* 2000;**44**:191.
15 **Kigasawa K,** Mashima Y, Ogata T, *et al.* A histopathological study of corneal amyloidosis secondary to trichiasis. *Nippon Ganka Gakkai Zasshi* 1996;**100**:394–400.
16 **Ando Y,** Nakamura M, Kai H, *et al.* A novel localized amyloidosis associated with lactoferrin in the cornea. *Lab Invest* 2002;**82**:757–66.
17 **Okuda T,** Matsumoto K, Ando Y, *et al.* A case of corneal lactoferrin amyloidosis secondary to trichiasis. *Nippon Ganka Gakkai Zasshi* 2003;**107**:105–8.
18 **Madisen L,** Hoar DI, Holroyd CD, *et al.* DNA banking: the effects of storage of blood and isolated DNA on the integrity of DNA. *Am J Med Genet* 1987;**27**:379–90.
19 **Orita M,** Suzuki Y, Sekiya T, *et al.* Rapid and sensitive detection of point mutations and DNA polymorphisms using the polymerase chain reaction. *Genomics* 1989;**5**:874–9.
20 **Kim SJ,** Yu DY, Pak KW, *et al.* Structure of the human lactoferrin gene and its chromosomal localization. *Mol Cells* 1998;**8**:663–8.
21 **El-Salhy M,** Suhr O. Endocrine cells in rectal biopsies from patients with familial amyloidotic polyneuropathy. *Scand J Gastroenterol* 1996;**31**:68–73.
22 **Klintworth GK,** Valnickova Z, Kielar RA, *et al.* Familial subepithelial corneal amyloidosis-a lactoferrin-related amyloidosis. *Invest Ophthalmol Vis Sci* 1997;**38**:2756–63.
23 **Baker EN,** Anderson BF, Baker HM, *et al.* Three-dimensional structure of lactoferrin. Implications for function, including comparisons with transferrin. *Adv Exp Med Biol* 1998;**443**:1–14.
24 **Tsunoda I,** Awano H, Kayama H, *et al.* Idiopathic AA amyloidosis manifested by autonomic neuropathy, vestibulocochleopathy, and lattice corneal dystrophy. *J Neurol Neurosurg Psychiatry* 1994;**57**:635–7.
25 **Tsujikawa M,** Kurahashi H, Tanaka T, *et al.* Identification of the gene responsible for gelatinous drop-like corneal dystrophy. *Nat Genet* 1999;**21**:420–3.
26 **Tasa G,** Kals J, Muru K, *et al.* A novel mutation in the M1S1 gene responsible for gelatinous droplike corneal dystrophy. *Invest Ophthalmol Vis Sci* 2001;**42**:2762–4.
27 **Stewart H,** Black GC, Donnai D, *et al.* A mutation within exon 14 of the TGFBI (BIGH3) gene on chromosome 5q31 causes an asymmetric, late-onset form of lattice corneal dystrophy. *Ophthalmology* 1999;**106**:964–70.